Offset Tolerant Hybrid Demodulator in Presence of a Wide Filter

Torben de Vries
University of Twente, Radio Systems
Enschede, the Netherlands
t.devries-1@student.utwente.nl

***Abstract*—The offset tolerant hybrid demodulator is robust against carrier frequency offset, but the receiver requires a wider filter to capture that offset. Previously, a shifted correlation method has been proposed in a double differential PSK demodulator to combat the extra noise added by the wide filter. The proposed demodulator in this paper combines the shifted correlations method with the offset tolerant hybrid demodulator. The results show that the shifted correlation method substantially improves the performance of the demodulator in presence of a wide filter. For a filter bandwidth that can tolerate frequency offsets up to 50 times the symbol rate, the shifted correlation method reduces the $E_b/N0$ required for $BER = 10^{-3}$ by 3dB for 2PSK/4FSK and 1.5dB for 4PSK/2FSk.**

I. Introduction

The ultra-narrow band (UNB) communication scheme is an attractive approach to low symbol rate communication in long range and interference rich applications [1]. UNB has become more popular for Machine-To-Machine (M2M) communications and Low Power Wide Area (LPWA) communications thanks to the advancements in signal processing [2]. The Hybrid FSK/PSK demodulator [3] has been proposed to increase the bit-rate with a different power and bandwidth efficiency trade-off compared to a higher order PSK and higher order FSK. The primary motivation behind the increase in bit-rate is to decrease the packet time. The increase in packet size might results from different coding technique that require transmitting extra bits to improve on the reliability of packet detection. A smaller modulation order will lead to a higher packet time if the symbol rate stays constant, which increases the time the receiver and transmitter are on and will lead to higher power consumption. An increase in PSK order will degrade the BER rate and exclusively using FSK results in a larger bandwidth which defies the whole purpose of UNB. One solution is hybrid modulation that uses combinations of MPSK and LFSK. The hybrid modulation is more power efficient than higher order PSK and more bandwidth efficient than higher order FSK.

One of the prominent challenges of UNB communication systems is carrier frequency offset (CFO) [4]. CFO is a result of mismatch between the receiver and the transmitter or the relative movement between them. It means that the receiver experiences a different carrier frequency than expected, and it is unable to detect and demodulate the signal. This can be solved with an offset tolerant hybrid demodulator proposed in [3]. It uses differential detection for FSK and double differential detection for PSK. Such usage of differential modulation requires that the phase has to be encoded *double differentially* and the frequency *differentially*.

The differential and double differential detection will remove the influence of the CFO, however, the receiver has to be equipped with a wider filter to capture the signal even in presence of a large CFO. This wide filter will result in an increase in the noise bandwidth and hence, a degradation of the BER performance.

A shifted correlation method is proposed in [5] that deals with the negative effects of a wider filter for a double differential PSK demodulator (DDPSK). The hybrid demodulator in [3] and the DDPSK demodulator in [5] are both based on autocorrelation; therefore, the question is whether the same method can be implemented for the hybrid demodulator to reduce the effect of wide filter. In this work the shifted correlation method is applied to the hybrid demodulator and its BER performance in presence of wide filter is evaluated.

The paper is structured as follows. First the hybrid demodulator in [3] and the shifted correlated method from [5] will be explained and analysed in sections II and III, respectively. After that, the proposed demodulator is presented in section IV. In section V, the results are included and it is discussed how far the method can help us overcome the wide filter problem. In the section VI, concluding remarks are presented.

II. Hybrid Demodulator

The demodulator introduced in [3] is a hybrid frequency and phase shift keying receiver. The receiver is a combination of Double Differential PSK and Differential FSK and is explained in the following.

A. Operation

The building blocks of the demodulator will be briefly mentioned and explained here as they form basis of the block diagram of the proposed demodulator. The block diagram of the offset tolerant hybrid demodulator is shown in Fig. 1.

The different subsections will also show the equations and effects on the signals. The baseband signal model at the receiver is as follows.

$$s_{k,n} = \sqrt{E_s/N_0} exp[j((\omega_n + \omega_0)((n-1)T + kTs) + \varphi_n)] \quad (1)$$

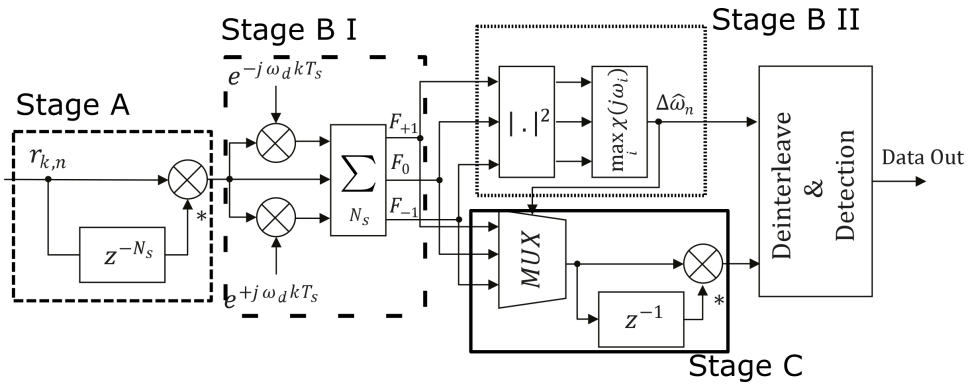

Fig. 1. Conventional Hybrid Demodulator

Here Es is the energy per symbol, N_0 is the noise density, ω_n is the frequency modulation with n being the symbol index, T is the symbol period, Ts is the sample frequency, k the sample index and φ_n the modulated angle information.

1) Stage A (first correlation): This stage in the block diagram is the first autocorrelation in the receiver design. This is what makes the receiver differential. This will result in:

$$\begin{aligned} X_{k,n} = \; & s_{k,n}s^*_{k,n-1} \\ & = \frac{E_s}{N_0} exp[j(\Delta\omega_n kTs + \Delta\omega_n(n-1)T \\ & + (\omega_{n-1}+\omega_0)T + \Delta\varphi_n)] \end{aligned} \tag{2}$$

In terms of (1) the indexing changed from n to $n-1$ and that will be multiplied with the conjugate of (1). The term $\Delta\omega_n(n-1)T$ can be ignored because the difference between the two modulated frequencies $\Delta\omega_n$ is always equal to the 2π times the symbol rate R_s or zero. This is a result of the value of frequency separation in FSK modulation which is equal to the symbol rate. Thus, because $1/R_s = T$ the term $\Delta\omega_n(n-1)T$ is a multiple of 2π

The first correlation stage transformed the modulated phase information into a difference in phase information of two consecutive symbols and made the frequency independent of ω_0; however, the frequency modulation and frequency offset is now present as a constant phase.

2) Stage B (filtering) & Stage B II (frequency estimation): The filter operates by mixing the signal with the possible values for $\Delta\omega_n = 0, \pm\,\omega_d$, where ω_d is the different frequency separation of FSK modulation. The frequency difference that matches the frequency part of the signal after the first autocorrelation stage, will down-covert the signal to DC. After the signal is integrated which acts like a lowpass filter, the MAX operator will choose the branch that has highest absolute magnitude, that will be the branch that has its frequency down-converted. This method correspond to calculating the DFT for the different possible frequencies. The frequency difference $\Delta\omega_n$ that corresponds to that branch is then called $\Delta\hat{\omega}_n$. The branch $\mathcal{X}_n(j\Delta\hat{\omega}_n)$ with the correct $\Delta\hat{\omega}_n$ is as follows.

$$\mathcal{X}_n(j\Delta\hat{\omega}_n) = E_s exp[j(+(\omega_{n-1}+\omega_0)T + \Delta\varphi_n))] \tag{3}$$

3) Stage C: This stage is mainly responsible for the PSK detection part and will use the results from the stage B II. Using the estimated frequency difference ($\Delta\hat{\omega}_n$) the MUX selects the correct path to continue with the signal, which has the same form as (3). As stated in the first autocorrelation stage, the modulated frequency and frequency offset have been transformed into a phase offset and will make it impossible to correctly determine the information that was transmitted using phase modulation. Similar to the first autocorrelation stage, the output of the MUX block is multiplied by the conjugate of its delayed version as follows.

$$\mathcal{X}_n(j\Delta\hat{\omega}_n)\mathcal{X}_{n-1}(j\Delta\hat{\omega}_{n-1})^* = E_s exp[j((\Delta\omega_{n-1})T + \Delta\varphi_n^2))] \tag{4}$$

$(\Delta\omega_{n-1})T$ is a multiple of 2π and can be neglected as explained before. Now the output of the second correlation only depends on the modulated phase.

$$D_n = exp[(j\Delta\varphi_n^2)] \tag{5}$$

B. Filter Bandwidth, CFO and sampling frequency

This paper will make frequent statements about filter bandwidth, symbol rate and sampling frequency. Fig. 2 shows the relation of the filter bandwidth **F** and the sampling frequency f_s. The filter bandwidth represented with the dashed line is able to capture the frequency in baseband up until the half the sampling frequency. Any frequency offset $\widehat{\Delta f}$ larger than $\widehat{\Delta f_1}$ are impossible for the receiver to demodulate. The sampling frequency is assumed to be a multiple of the symbol rate. $F_s = N/R_s$. This also means that the filter bandwidth is limited to half the amount and with that, the filter bandwidth is proportional to N. To summarize, any specific number N means that the sampling frequency is N times the symbol rate and that the filter bandwidth can tolerate half of that as a maximum frequency offset, the maximum carrier frequency offset is $\widehat{\Delta f_1}$. In the rest of this paper we present results and performance evaluations in terms of the value N.

III. Shifting Correlations

A. Method

The paper [5] proposed a novel method to combat the BER performance degradation that is caused by the extended noise

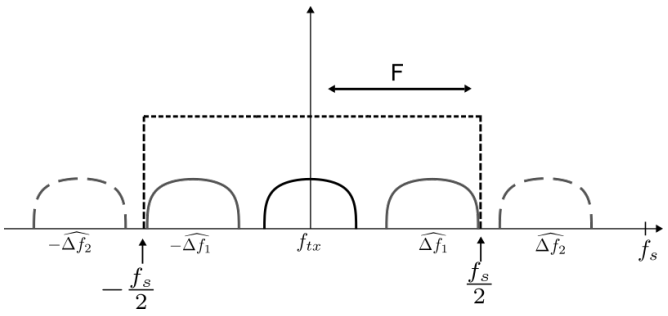

Fig. 2. Visualization of wider filter.

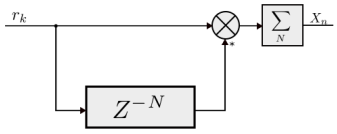

Fig. 3. Conventional autocorrelation.

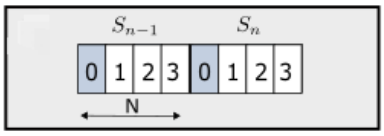

Fig. 4. Symbols and their samples.

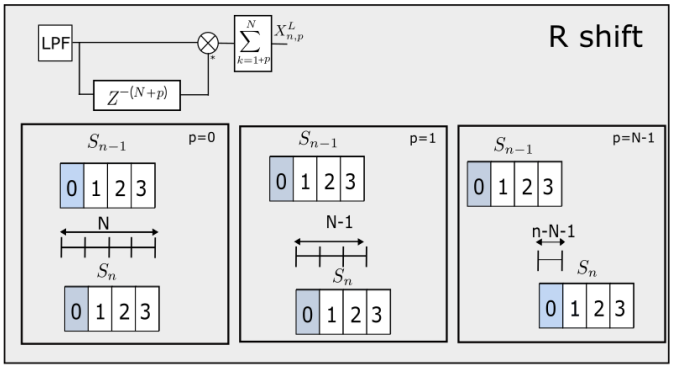

Fig. 5. Shifing Right.

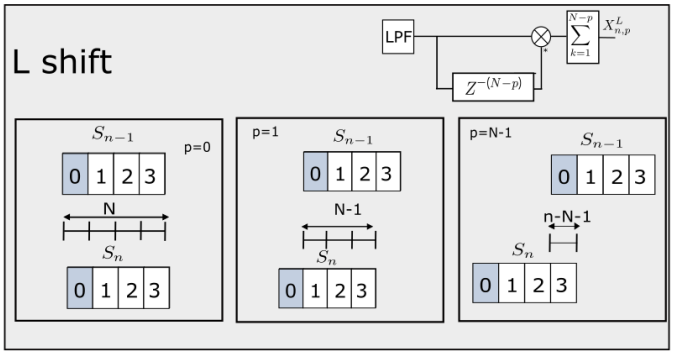

Fig. 6. Shifing Left.

bandwidth. It introduces a double differential demodulator in which the first correlation shifts between the samples of the delayed version. In a conventional method the correlation can be shown as a block diagram as in Fig. 3. The current symbol is multiplied with the conjugate of its delayed version. In the conventional method the symbol is delayed by exact numbers of samples per symbol; whereas, in the proposed method, the previous symbol is not delayed by an entire symbol but rather by fewer or more samples than the number of samples per symbol. The Fig. 4, Fig. 6, Fig. 5 and the subsection **Shifting Example** show an example of the shifted correlations for symbols that consist of four samples.

B. Shifting Example

The Fig.4 shows the two symbols of interest, the previous one S_{n-1} and the most recent one S_n. N indicates the number of samples that make up one symbol. A larger number N also corresponds to a wider filter which requires more samples of the same symbol.

Fig. 5 and Fig. 6 show the right shift and the left shift, respectively. These are the two possibilities, namely a shift in samples to the right and a shift to left from the perspective of the current symbol. The number p indicates the amount of the shift, with $N-1$ being the largest shift as it results into only one output sample.

C. Working principle

One of the requirements of this technique is the independence of the noise samples. This is guaranteed when the sampling frequency is chosen as in Section IV B. As we earlier explained, filter bandwidth and sampling frequency are related and because the sampling frequency is N times larger than the actual symbol rate, the demodulator will end up with $N = F_s R_s$ complex samples for every symbol. This concept refers back to the Fig. 2 and the section belonging to it. The samples of the received signal have the mathematical form of:

$$r_{k,n} = s_{k,n} + \eta_{k,n} \tag{6}$$

k is the sample index and n the symbol index. The signal is modelled as a rectangular pulse shape and hence, the signal components $s_{k,n}$ do not change for different k, while the noise samples $\eta_{n,k}$ are independent random variables. At the output of the first stage of autocorrelation we have:

$$\begin{aligned} X_{k,n} =& s_{k,n}s_{k-p,n-1} + s_{k,n}\eta_{k-p,n-1} + s_{k-p,n-1}\eta_{k,n} \\ &+ \eta_{k,n}\eta_{k-p,n-1} \end{aligned} \tag{7}$$

This means that when correlating the different combinations of the complex symbols in the receiver the signal and noise add up differently because of their coherence. The first three terms in the summation are correlated for different p , the last one, which is noise-by-noise multiplication, is uncorrelated for different paths (p values). This means that the SNR with respect

to the last noise component will improve if all the decision variables from different p paths are added together. A more elaborate and mathematical analysis of shifted correlation and how it improves the performance can be found in the paper [5].

IV. Proposed demodulator

In this section, the demodulator will be presented. It has been developed to combat the problem of a wide filter in the hybrid offset tolerant demodulator. In this section, first, the mathematical expressions are derived and explained. Afterwards, one of the problems with the shifting correlation will be described and a solution is provided. At last, the block diagram of the proposed demodulator is introduced and explained.

A. mathematical derivation

Similar to the hybrid offset tolerant demodulator (1), the received baseband signal can be modelled as:

$$s_{k,n} = \sqrt{E_s/N_0} exp[j((\omega_n + \omega_0)((n-1)T + kTs) + \varphi_n)] \tag{8}$$

The main path can be achieved similar to (1) from the conventional hybrid method. For a path with shifted correlation, the shift in the sample index *k* in the conjugate of the delayed version of the signal is different from the main path. Here, we focus our derivations on the R shift shown in Fig. 5. the same procedure can be followed for L shift. The R shift is considered; thus, the shift is presented as a minus p and $s^*_{k-p,n-1}$ is as follows.

$$s^*_{k-p,n-1} = \sqrt{E_s/N_0} exp[-j((\omega_{n-1} + \omega_0)((n-2)T + (k-p)Ts) + \varphi_{n-1})] \tag{9}$$

The autocorrelation in path p is defined as:

$$s_{k,n} s^*_{k-p,n-1} = X^R_{k-p,n} \tag{10}$$

Taking (8) and (9). This autocorrelation will result in:

$$X^R_{k-p,n} = E_s/N_0 exp[j(\Delta\omega_n(n-1)T + (\omega_{n-1} + \omega_0)T + \Delta\omega_n kTs + (\omega_{n-1} + \omega_0)(p)Ts + \Delta\varphi_n)] \tag{11}$$

The term $\Delta\omega_n(n-1)T$ can be ignored as it is a multiple of 2π. This is the same as in the section **Hybrid Demodulator**. The equation then simplifies to:

$$X_{k-p,n} = E_s/N_0 exp[j((\omega_{n-1} + \omega_0)T + \Delta\omega_n kTs + (\omega_{n-1} + \omega_0)(p)Ts + \Delta\varphi_n)] \tag{12}$$

Considering that $T = NTs$ we can rewrite the equation as follows.

$$X_{k-p,n} = E_s/N_0 exp[j((\omega_{n-1} + \omega_0)(N+p)Ts + \Delta\omega_n kTs + \Delta\varphi_n)] \tag{13}$$

B. frequency Detection

After the first multiplication, the frequency is independent of the frequency offset and can be used to detect the information contained in the frequency difference of two consecutive symbols. The procedure is equal to the conventional hybrid demodulator. The mathematical expression for the max operator is as follows:

$$\Delta\hat{\omega}_n = max|\mathcal{X}(j\omega_i)|^2 \tag{14}$$

$\mathcal{X}(j\omega_i)$ is the product of the first autocorrelation with frequencies equivalent to the different possible $\Delta\omega_n$. The $\Delta\omega_n$ that has been chosen as the max is $\Delta\hat{\omega}_n$, and the correct branches are as follows.

$$\mathcal{X}(j\Delta\hat{\omega}_n) = \sum_{k=0}^{N_s-1} X_{n,k} exp[-j\Delta\hat{\omega}_n kT_s] \tag{15}$$

$$= E_s exp[j((\omega_{n-1} + \omega_0)T + \Delta\varphi_n)] \tag{16}$$

This Operation changes its summation boundaries based on which path delay in sample index is used. For R path it is:

$$\mathcal{X}^R(j\Delta\hat{\omega}_n) = \sum_{k=0}^{N_s-p-1} X_{n,k-p} exp[-j\Delta\hat{\omega}_n kT_s] \tag{17}$$

$$= E_s exp[j((\omega_{n-1} + \omega_0)(N+p)T_s + \Delta\varphi_n)] \tag{18}$$

and for the L shift

$$\mathcal{X}^L(j\Delta\hat{\omega}_n) = \sum_{k=p}^{N_s-1} X_{n,k+p} exp[-j\Delta\hat{\omega}_n kT_s] \tag{19}$$

$$= E_s exp[j((\omega_{n-1} + \omega_0)(N-p)T_s + \Delta\varphi_n)] \tag{20}$$

C. Second Multiplication/correlation

After the frequency has been detected and the correct signal has been chosen from the different possible paths corresponding to $\Delta\omega_n$, the signal will be autocorrelated a second time. The signal at the output of the selected branch is:

$$\mathcal{X}^R_{n,p} = E_s exp[j((\omega_{n-1} + \omega_0)(N+p)T_s + \Delta\varphi_n)] \tag{21}$$

And the delayed version is:

$$\mathcal{X}^R_{n-1,p}{}^* = E_s exp[-j((\omega_{n-2} + \omega_0)(N+p)Ts + \Delta\varphi_{n-1})] \tag{22}$$

The multiplication then results into:

$$\mathcal{X}^R_{n,p}\mathcal{X}^R_{n-1,p}{}^* = E_s exp[j((\Delta\omega_{n-1})(N+p)T_s + \Delta^2\varphi_n)] \tag{23}$$

As explained earlier, in the conventional hybrid path, the term $\Delta\omega_{n-1}(N)Ts$ is a multiple of 2π and becomes zero. The resulting equation is:

$$D^R_{n,p} = E_s exp[j((\Delta\omega_{n-1})pT_s + \Delta^2\varphi_n)] \tag{24}$$

D. phase correction

The shifted signals add an unwanted phase shift to the signal as can be seen from (24) The unwanted phase $(\Delta\omega_{n-1})pTs$ depends on the symbol period, the shift in the autocorrelation from the first differential stage and the frequency difference of the two previous symbols. The symbol period and the amount of shift are known design constants and the frequency difference of the two previous symbols is also the output of the frequency detection. Therefore, the information, which is used to select the correct signal at the MUX can also be used to eliminate the unwanted phase offset.
After the phase correction is applied to the signal, the equation is as follows.

$$D_{n,p}^{R} = E_s exp[j((\Delta^2\varphi_n)] \tag{25}$$

The phase can now be estimated by the detection part.

E. block diagram

The block diagram of the demodulator is depicted in Fig. 7. The block diagram that is presented is made to demodulate 2FSK/4PSK signals. This work also presents the results for different combinations of hybrid demodulators, but higher FSK requires more branches and will make the diagram unreadable. The received baseband signal (8) is split into three branches, one conventional path and two sets of shifted paths, all three pass through an autocorrelation stage, with the two shifted paths having their autocorrelation stage modified based on their shift p. Afterwards, the signals pass through the filter stage. The filter stage starts with splitting the signal into three branches with different mixing coefficients, which are equivalent to the various frequency differences. Additionally, the filter stage has a summation over the samples. This summation means that after the filter stage the signal has only a symbol index and for the shifted paths also a p index which indicates the amount of the shift. After the filters each path has two sections; FSK detection which is the top one and the PSK detection which is the bottom one. This is indicated in the block diagram with the two boxes. To detect the FSK, the absolute value squared is taken and summed up over all paths p and over the three different autocorrelations outputs (conventional, right shift and left shift). After that, the frequency detection is done in the MAX block. The result of the MAX block is also used to select the proper path which goes to the next stage of differential decoding. The signal in the adequate branch looks like (16) for the conventional path and like (18) and (20) for the right shift and the left shift, respectively. The next step is the second autocorrelation stage, which is the same for all the shifts p, but the difference is that the two shifted parts need their phase correction and after that their decision variables need to be summed up over all p shifts. After the summation over p, the three different shifting path are summed up, and together with the output of the MAX-block, the detection block can provide the transmitted data.

V. Results and Discussion

In this section, we show the simulation results and findings of the proposed demodulator. The first part will feature graphs that show the BER degradation for different combinations of PSK and FSK. After that, we will continue with the improvement that the new demodulator can achieve. The implementation and simulation of the receiver are done in the MatLab environment. The signals are modelled in an AWGN channel.
In the next part, different combinations of MPSK and LFSK and different sizes of filter are demonstrated. The filter bandwidth is described in terms of N. This refers back to section III B. Any number for N means that the sampling frequency is $f_s = NR_S$. The filter bandwidth than goes to half of that value and consequently, the number of complex samples per symbol is N, and with increasing N more paths can be used, but to avoid long simulation times, we have used up to only 5 paths.

A. Effect of a wider filter

First the effect of a wider filter is shown in Fig. 8 and Fig. 9 and how it degrades the BER performance for 2PSK/2FSK (fig.8) and 4PSK/2FSK (fig.9).
The graphs show that for different combinations of PSK and FSK, the effect of a wider filter varies. The wider filter has less impact on the 4PSK/2FSK performance than for the 2PSK/2FSK one. The negative effect on the BER performance will decrease with an increase in the PSK order. This effect occurs because the distance between the different constellations points reduces. To refer back to (7) this means that the second and third terms dominate the overall noise and the fourth term, which is mainly from the increase in noise bandwidth, is less dominant in the overall BER performance. When N is increased from 10 to 100 at 10^{-3}, the 2PSK/2FSK becomes 3dB worse, while this difference is 1.5 dB for 2FSK/4PSK.

B. Effects of paths

In this section, we are going to have a look at the different combinations of PSK and FSK and how the proposed demodulator can achieve a better BER performance. The graphs show a dashed line with a description of "reference". The reference is made with the LFSK/MPSK combination for $N = 10$. The amount of paths is always zero for the reference curve. This reference curve can be seen as the BER performance of the conventional hybrid demodulator. This section talks about paths and shifts frequently, which essentially mean the same, as they both describe the amount of shift in samples during the shifted autocorrelation. Some paths have the possibility to get a better performance than the reference value, this makes sense as even $N = 10$, which is used for the reference, has some noise-by-noise components in every symbol. This means that the reference curve is not a theoretical value or a curve that the paths approximate. This fact does not make the reference value less helpful in determining the effectiveness of the paths. It gives a indication of how the conventional offset tolerant demodulator would perform with a filter bandwidth

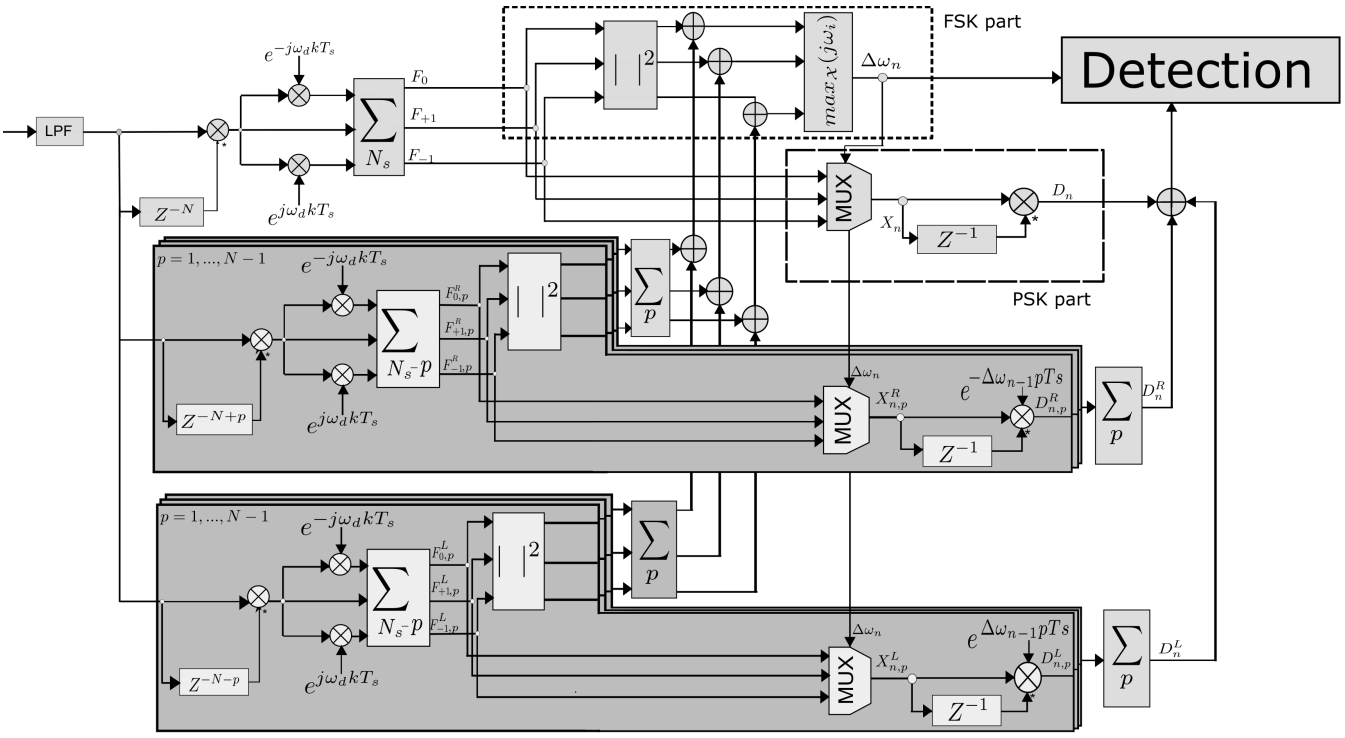

Fig. 7. proposed Hybrid Demodulator

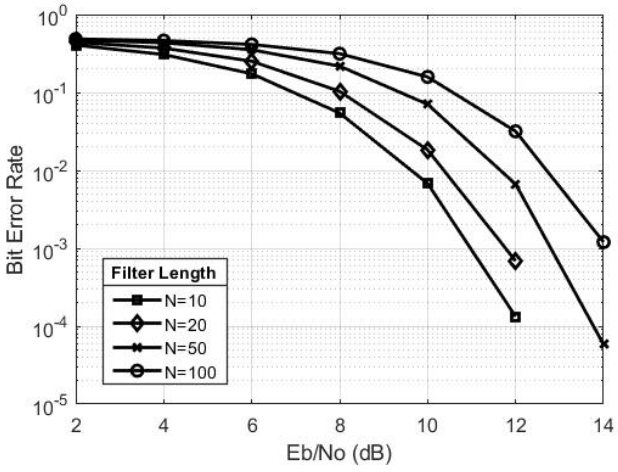

Fig. 8. 2PSK, 2FSK in presence of a wide filter

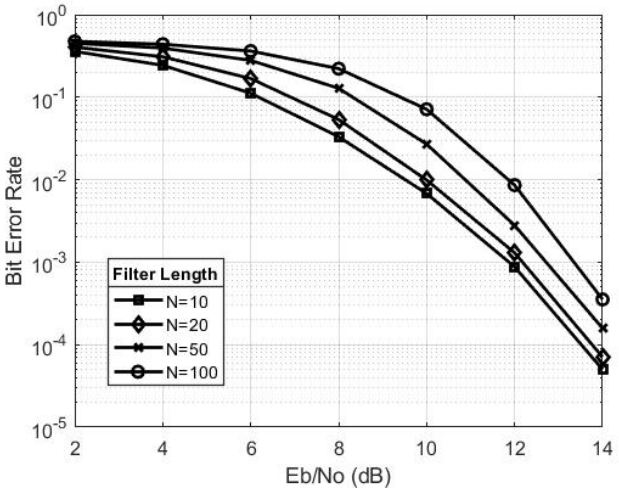

Fig. 9. 4PSK, 2FSK in presence of a wide filter

of $N = 10$ compared to the MPSK/LFSK combinations with different filter bandwidths.

Fig. 11 shows 2PSK/2FSK in presence of a wide filter $N = 100$ and p is the number of paths. It also shows the impact of changing p on the BER performance. The addition of one path gives an improvement of approximately 1dB at 10^{-3}, and a shift of 4 gives about 1.5dB improvement at 10^{-3}. The first path has a more significant impact on the BER performance than the following p values. This impact is because, for a smaller p more of the samples of one symbol are used in forming the resulting decision variable of that path. After the first auto-correlation stage, the output samples are summed and averaged, so more samples that overlap results in decision variables that influence the BER performance more significantly. Fig. 10 presents the combination of 4PSK/2FSK

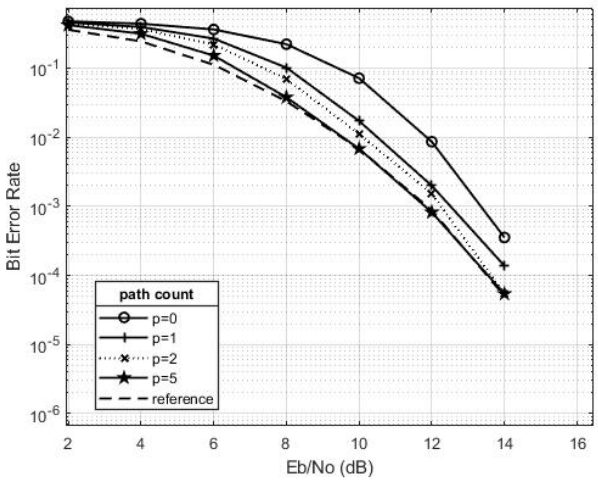

Fig. 10. 4PSK, 2FSK in presence of a wide filter(N=100) and different paths

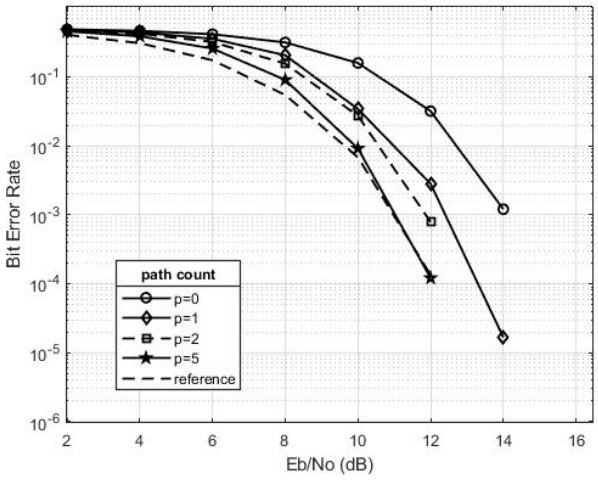

Fig. 11. 2PSK, 2FSK in presence of a wide filter (N=100) and different paths

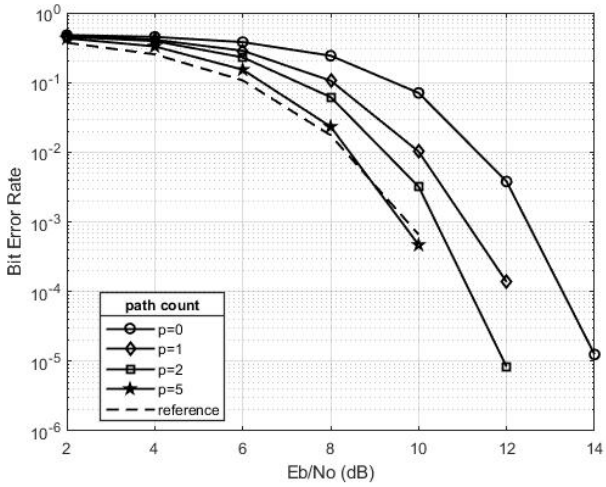

Fig. 12. 2PSK, 4FSK in presence of a wide filter (N=100) and path effects of different path number

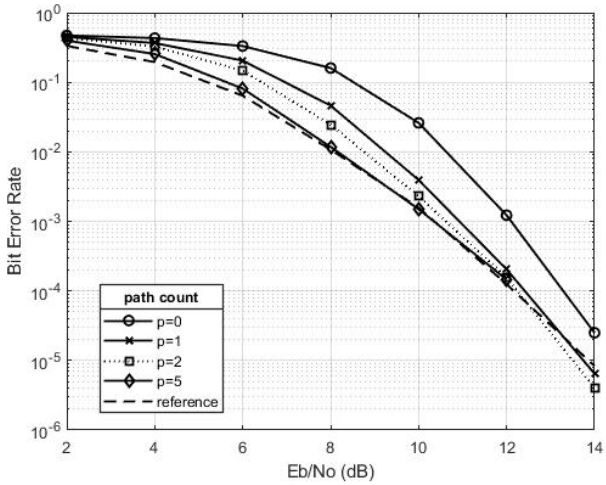

Fig. 13. 4PSK, 4FSK in presence of a wide filter (N=100) and path effects of different path number

with the effects of additional paths. As earlier mentioned, the impact of the wider filter is less prominent in a higher PSK scheme, and hence, the addition of more paths does not improve the performance as significantly as in 2PSK/2PSK. The reference curve is worse than the one for 2PSK 2FSK. It shows that the performance of the demodulator that the path approximate is dependent on the modulation scheme.

Fig. 12, which is 2PSK/4FSK, is similar to the 2PSK/2FSK situation. The effects of a wide filter is more prevalent in a lesser PSK scheme and the improvement that the paths can obtain are much higher than for higher PSK modulation The last combination, which is 4PSK/4FSK, is shown in Fig. 13. The same conclusion as with 2FSK/4PSK can be derived. The wider filter has less impact on the overall BER performance than for smaller PSK order and additional path offer less improvement. Nonetheless, even the improvement that can be achieved for 4PSK and 4FSK is about 2dB. In summary, all the combinations get close and sometimes surpass the reference value. This means that the BER performance of the proposed demodulator in presence of a wide filter (N=100) matched the conventional hybrid demodulator with an amount of 5 paths. The effects of more paths than 5 will then most likely outperform the reference curve.

The graphs that have been discussed so far have a sampling frequency equal to 100 times the symbol rate,which means that they can tolerate a frequency offset close to 50 times the symbol rate. The next graphs will show the effects of a path for a filter that are less than 100 times the symbol rate. With a filter bandwidth of with $N = 20$, the paths are more likely to surpass the reference curve.

Fig. 14 shows the BER curves for 4PSK/2FSK for a sampling frequency that is 20 times the symbol rate. To review, after the first path, the BER curve has a better performance than the

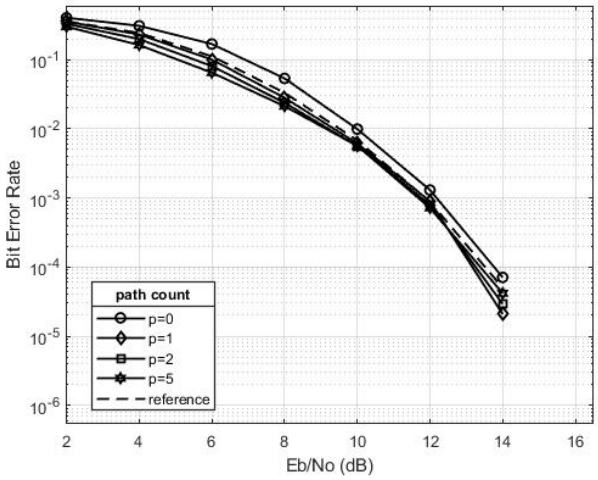

Fig. 14. 4PSK, 2FSK in presence of a wide filter (N=20) and path effects of different path number

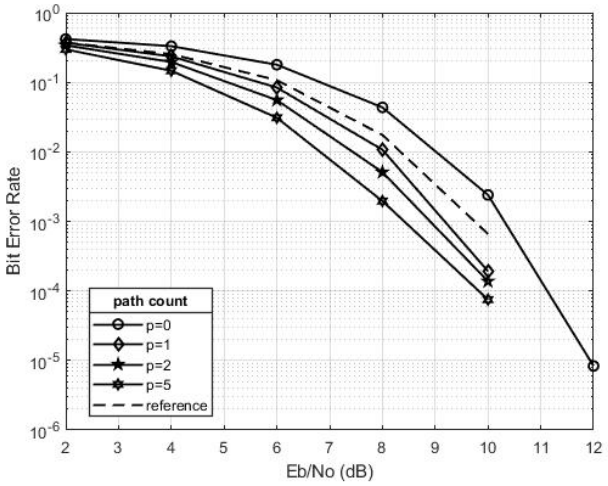

Fig. 15. 2PSK, 4FSK in presence of a wide filter (N=20) and path effects of different path number

reference value. However, there is only a slight improvement in BER performance after the first path and the next path do not stray far apart from the reference curve.

Furthermore, Fig. 15 shows the 2PSK/4FSK BER performance for a filter bandwidth that is 20 times the symbol rate. The reference value shown for 2PSK/4FSK, which was created with a filter bandwidth that can tolerate 10 times the symbol rate as frequency offset, is outperformed after the first path and path 5 shows greater improvement than path 5 for Fig. 14, more paths than 5 are still likely to result in more improvement for 2PSK/4FSK.

In summary, a filter bandwidth with $N = 20$ for higher PSK has little effect on the degradation. On the contrary, a wide filter with only 20 time the symbol rate for higher FSK can still acquire an improvement of approximately 2dB, as can be seen for 10^{-3} in the Fig. 15. Increasing the order of FSK adds an orthogonal dimension to the constellations diagram. In contrast, higher-order PSK makes the constellations diagram more crowded and result in the degradation of the BER performance, regardless of the filter bandwidth.

VI. Conclusion

The technique of hybrid modulation and shifted correlation has been analysed to design a system that can overcome the negative effects of a wide filter. The paper shows that the effects of a wider filter vary for different modulation orders, and so does the improvement that shifted correlation can offer. However, performance improvement is visible, at 10^{-3} and N=100 (a filter bandwidth equal to 50 times the symbol rate), for combinations with 2PSK we can obtain a performance boost of 3dB and for 4PSK up to 1.5dB. The results indicate that the offset tolerant hybrid demodulator for any combination of MPSK/LFSK and any filter bandwidth can be improved with this technique.

Acknowledgment

I would like to express my appreciation to my supervisor Siavash for his guidance and persistent help throughout this assignment. I am also indebted to Siavash for providing the code to the hybrid and DDPSK demodulators, which are the basis of this thesis.

References

[1] K. E. Nolan, W. Guibene, and M. Y. Kelly, “An evaluation of low power wide area network technologies for the internet of things,” in 2016 International Wireless Communications and Mobile Computing Conference (IWCMC), Conference Proceedings, pp. 439–444.

[2] M. Anteur, V. Deslandes, N. Thomas and A. Beylot, ”Ultra Narrow Band Technique for Low Power Wide Area Communications,” 2015 IEEE Global Communications Conference (GLOBECOM), San Diego, CA, 2015, pp. 1-6, doi: 10.1109/GLOCOM.2015.7417420.

[3] S. Safapourhajari and A. B. J. Kokkeler, ”Offset Tolerant Demodulator for Frequency/Phase Modulation in Time-Varying Channel,” 2019 IEEE Wireless Communications and Networking Conference (WCNC), Marrakesh, Morocco, 2019, pp. 1-6, doi: 10.1109/WCNC.2019.8886086.

[4] D. Lachartre, F. Dehmas, C. Bernier, C. Fourtet, L. Ouvry, F. Lepin, E. Mercier, S. Hamard, L. Zirphile, S. Thuries, and F. Chaix, “7.5 a tcxo-less 100hz-minimum-bandwidth transceiver for ultra-narrow-band sub-ghz iot cellular networks,” in 2017 IEEE International Solid-State Circuits Conference (ISSCC), ISSCC, Conference Proceedings, pp. 134–135.

[5] S. Safapourhajari and A. B. J. Kokkeler, “Demodulation of double differential psk in presence of large frequency offset and wide filter,” in 2018 IEEE 87th Vehicular Technology Conference (VTC Spring), siavash, Conference Proceedings, pp. 1–5.